Int. J. Electrochem. Sci., 7 **(2012)** 6941 - 6950

International Journal of
ELECTROCHEMICAL
SCIENCE
www.electrochemsci.org

Utilizing of Sodium Nitrite as Inhibitor for Protection of Carbon Steel in Salt Solution

Maan Hayyan[1,*], *Shatha A. Sameh*[2], *Adeeb Hayyan*[1], *Inas M. AlNashef*[3]

[1] Department of Chemical Engineering, Faculty of Engineering, University of Malaya, Kuala Lumpur, 50603, Malaysia
[2] Department of Chemical Engineering, University of Technology, Baghdad, Iraq
[3] Chemical Engineering Department, King Saud University, Riyadh, Saudi Arabia
[*]E-mail: maan_hayyan@yahoo.com

Received: 30 May 2012 / *Accepted:* 28 June 2012 / *Published:* 1 August 2012

Preventing corrosive action induced by the presence of chlorine in utility water used as a coolant in cooling towers is a challenging task. Anodic inhibition is one of the commonly used techniques for protecting metallic parts of the cooling towers. In this study, the effect of chloride ions on the sodium nitrite ($NaNO_2$) inhibitor concentration was investigated for the protection of carbon steel pipes under controlled conditions of mass transfer. A rotating cylinder electrode system was utilized to provide quantified hydrodynamic mass transfer conditions. Potentiostatic polarization experiments were carried out at 313 K and rotational speeds of 0, 200, 350 and 500 rpm. It was selected a typical industrial chloride solution at a concentration of 250 ppm *NaCl*. The experiments were conducted in the presence of $NaNO_2$ with different concentrations depending on the $[NaNO_2/NaCl]$ molar ratio, i.e. ratios of 0 to 1. A new calculation was used to find the best protection value which depends on the passive film stability in the polarization curve. The current analysis revealed that the new method for predicting the optimum protection value is more reliable than the conventional corrosion current density based technique.

Keywords: carbon steel, anodic inhibition, sodium nitrite, passive film, polarization

1. INTRODUCTION

In the oil extraction and processing industries, inhibitors have always been considered to be the first line of defense against corrosion. A great number of scientific studies have been devoted to the subject of corrosion inhibitors [1]. Corrosion inhibitors are chemical substances or combination of substances that, when present in the environment, prevent or reduce corrosion [2].

Passivating inhibitors are one of the most important inhibitors [3]. This type of inhibitors is widely used because of its high effectiveness compared to other types of inhibitors [1]. It is especially effective on steels, copper base alloys and certain other alloy systems [4]. Passivators are the most efficient inhibitors used in cooling water system. These inhibitors lead to the rapid formation of a protective oxide film over the anodic sites on the metal corroding surface [3]. However, in general, passivation inhibitors can actually cause pitting and accelerate corrosion when concentrations fall below minimum limits [1]. For this reason, it must be used with caution [5].

Nitrite is one of the most commonly used anodic inhibitors, shifting the corrosion potential to more noble values and reducing corrosion current [3-6]. Sodium nitrite ($NaNO_2$) is classified as an anodic inhibitor and requires a critical concentration for the protection of steel [3, 7-9]. At low concentrations, the nitrite may create imperfect passivity and subsequently the corrosion will be increased. The chloride concentration is equally important since when the chloride/nitrite ratio is high, the passivity effect is lost [10].

With passivating inhibitors that contain $NaNO_2$, cathodic polarization curves for near-neutral solutions of these materials will intersect the anodic polarization curves for steels in the passive range and provide very low corrosion rates [5].

Stansbury and Buchanan [5] investigated the corrosion of iron in aerated (DO of 8.5 ppm) and deaerated (DO of ~1 ppm) environments and with nitrite additions at a pH=7. The corrosion rates were calculated for each condition to be:

- aerated (clean surface): 500 mA/m^2
- aerated (rust surface): 60 mA/m^2
- deaerated: 5 mA/m^2
- deaerated with nitrite ion: 1.8 mA/m^2
- aerated with nitrite ion: 1.4 mA/m^2

Matsuda and Uhlig [11] and Mercer *et al.* [12] have carried out extensive studies for the effects of different nitrite/chloride ratios, in aqueous solutions, on the corrosion behavior of mild steel. Their investigation revealed that for a pure chloride solution and a metal with the oxide film not removed, $[NaNO_2/NaCl]$ ratio of 0.4 was enough to provide complete protection and for objects from which the coating has been removed, the ratio was about 0.7.

On the other hand, it has been noticed that the protection is not observed for a 0.4 ratio of the $[NaNO_2/NaCl]$ concentrations. At ratios higher than 0.7, full protection was achieved. In some cases where steel was preliminarily kept in $NaCl$ and then treated with $NaNO_2$, protection was not afforded even at ratios as high as 0.7 to 2.0 [3]. Therefore, initially, the iron surface must be reasonably clean and free of corrosion products.

Conoby and Swain [13] reported that the nitrite level should be at least equal to that of the chloride and should exceed the sulfate by 250 to 500 mg/L. The protective oxide formed on the treated metal surface with nitrites consists mainly of Fe_3O_4 and γ-Fe_2O_3 [14,15]. Cohen [14] stated that to maintain the protectiveness of this film, it is necessary that the iron in the outer layer must be in the ferric or higher oxidation state. In the absence of an oxidizing agent, the film tends to revert to Fe_3O_4 by reaction with underlying metal. The oxidizing inhibitors and/or oxygen maintain the outer layer in the higher oxidation state. The film is very thin and typically 2×10^{-3} μm, and it is possibly formed

through the adsorption of the nitrite ions followed by an oxidation step. The overall reaction is one or both of the following reactions [16]:

A) Formation of lower oxide

$$NO_2^- + 8H^+ + 6e^- \rightarrow NH_4^+ + 2H_2O$$

$$9Fe(OH)_2 \rightleftarrows 3Fe_3O_4 + 6H_2O + 6H^+ + 6e^-$$

$$2H_2O \rightleftarrows 2H^+ + 2OH^-$$

$$9Fe(OH)_2 + NO_2^- \rightarrow 3Fe_3O_4 + NH_4^+ + 2OH^- + 6H_2O \qquad 1$$

B) Formation of higher oxide

$$NO_2^- + 8H^+ + 6e^- \rightarrow NH_4^+ + 2H_2O$$

$$6Fe(OH)_2 \rightleftarrows 2Fe_3O_4 + 4H_2O + 4H^+ + 4e^-$$

$$2Fe_3O_4 + H_2O \rightleftarrows 3(\gamma - Fe_2O_3) + 2H^+ + 2e^-$$

$$2H_2O \Leftrightarrow 2H^+ + 2OH^-$$

$$6Fe(OH)_2 + NO_2^- \rightarrow 3(\gamma - Fe_2O_3) + NH_4^+ + 3H_2O + 2OH^- \qquad 2$$

Joseph [16] presumed that in an aerated electrolyte ammonium ions are oxidized by oxygen with regeneration of nitrite ions according to the Eq 3.

$$NH_4^+ + H_2O + 1/2O_2 \rightarrow NO_2^- + 2H_2O + 2H^+ \qquad 3$$

The NO_2^- inhibits the pit formation and also can inhibit the formation of ferrous oxides while the formation of ferric oxides are enhanced as confirmed by previous studies [17,18].

2 EXPERIMENTAL DETAILS

2.1 Experimental apparatus

The experimental apparatus used in this work consisted mainly of a potentiostat (Wenking LT. 87) on-line with a computer by an A/D interface, polarization cell, rotating cylinder electrode assembly, digital multimeters and water bath with controlled temperature (Memert P21S6).

2.2 The working electrode (rotating cylinder)

The rotating cylinder electrode (RCE) comprised a carbon steel cylinder, which has the following dimensions: r_o = 15 mm, r_i = 8 mm, h = 20 mm. Thus, the surface area of the specimen was 18.84 cm^2. The spectrographic analysis of the carbon steel is given in Table 1.

Table 1. Spectrographic composition of carbon steel (wt %).

C	Mn	Si	Ni	S	Cr	Fe
0.1611	0.367	0.043	0.0225	0.0162	0.0033	99.3869

2.3 Experimental methodology

Potentiostatic experiments were carried out at 313K with controlled conditions of flow, i.e. 0, 200, 350 and 500 rpm for RCE. A single experiment involved electrochemical polarization of carbon steel electrode from – 0.9 V and scanned potentiostatically to the noble (positive) direction until breakdown was reached, with a scan rate of 20×10^{-3} V/min. The experimental procedure was repeated in the presence of $NaNO_2$ with different concentrations depending on the $[NaNO_2/NaCl]$ ratio, i.e. 0, 0.3, 0.4, 0.5, 0.6, 0.7, 0.8, 0.9 and 1, for 250 ppm of *NaCl*.

3. RESULTS AND DISCUSSION

The polarization curve, Fig 1, shows a plot of the electrode potential *vs.* the logarithm of the current density, and it can be noticed the regions which are elaborated in this study. The curve is marked, in order of increasing electrode potential as ABCDEF where:

AB: is the cathodic region.

B: corresponds to the corrosion potential (partial passive potential).

BCDEF: is the anodic region which includes:

- The partial passive region (pre-passivation) (BC), where (C) is the complete passive potential.
- The complete passive region (CD), where (D) is the breakdown potential.
- The active dissolution region (DE), where (E) is the second passive potential.
- The second passive region (Re-passivation) (EF).

The important characteristics of the anodic region are the partial passive potential (E_p), the complete passive potential, the complete passive current density (i_p), the breakdown potential and the breakdown current density. The effects of experimental variables changes on these characteristics are reported separately below.

3.1 The Cathodic Region (AB)

Since $NaNO_2$ is a good anodic inhibitor as stated previously [3, 7, 19-23], its effect was restricted to the anodic region only. Therefore, the cathodic current density was not reported in this study.

3.2 The Corrosion Potential (Partial Passive Potential) (B)

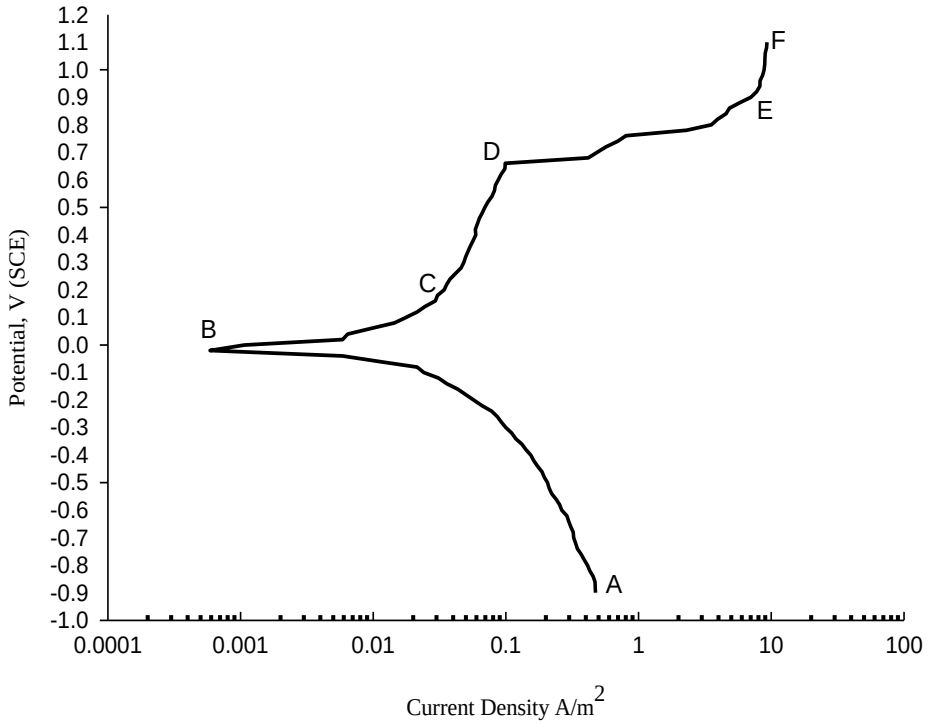

Figure 1. Potentiostatic polarization curves of carbon steel, inhibited solutions at conc. of *NaCl* = 250 ppm, $NaNO_2$ =175 ppm, ratio $[NaNO_2/NaCl]$ = 0.7, T = 313 K and 200 rpm.

It can be noticed that the corrosion potential values, in general, are nobler than those obtained under identical conditions in uninhibited solutions, as shown in Table 2. This confirms that $NaNO_2$ acts as a good anodic inhibitor. This regularity in the electrochemical behavior of steel is caused by the fact that the inhibitor produced a shift in the potential from the steady state value to the partial passivation potential which is governed mainly by the acceleration of the cathodic reaction. In contrast, the potential shift of the metal from that of partial passivation to that of complete passivation was already largely governed by the inhibition of the anodic reaction [3].

Table 2. The corrosion potential of inhibited solution, V.

rpm	[$NaNO_2$/NaCl]								
	0.0	0.3	0.4	0.5	0.6	0.7	0.8	0.9	1.0
0	-0.36	-0.30	-0.30	-0.28	-0.24	-0.10	-0.32	-0.10	-0.18
200	-0.34	-0.28	-0.24	-0.22	-0.16	-0.02	-0.26	-0.22	-0.14
350	-0.32	-0.24	-0.24	-0.22	-0.02	-0.12	-0.24	-0.07	-0.18
500	-0.30	-0.22	-0.10	-0.12	-0.12	-0.14	-0.22	-0.14	-0.14

3.3 The Complete Passive Region (CD)

3.3.1The Complete Passive Potential (C)

The results presented in Table 3 illustrate that the complete passive potentials in inhibited solution are very near to the partial passive potential ($E_{corr.}$). This enhances the technique which will be dependent on to evaluate (i_{corr}). When the potential of metal shifts away from the potential of partial passivation, the nitrite ions start to exhibit the passivating properties with respect to the anodic reaction. Therefore, the transfer of metal will be facilitated to pass to the passive state.

Table 3. The complete passive potential of inhibited solution, V.

rpm	[$NaNO_2$/NaCl]							
	0.3	0.4	0.5	0.6	0.7	0.8	0.9	1.0
0	-0.200	-0.220	-0.220	-0.120	0.020	-0.180	0.100	-0.080
200	-0.160	-0.160	-0.180	-0.080	0.120	-0.220	-0.140	-0.060
350	-0.200	-0.080	-0.140	0	-0.100	-0.140	0.020	-0.140
500	-0.140	-0.040	-0.040	0	-0.100	-0.160	-0.020	0.020

3.4 The Corrosion Current Density (i_{corr})

With *$NaNO_2$* inhibitor in chloride solution, the cathodic curve intersects the anodic curve in the passive region (BD), and consequently it can be considered that $i_{c.p.}=i_{corr}$, as depicted in Fig 1 [4,5]. In general, it can be noticed that the corrosion current density decreases drastically with increasing ratio of *[$NaNO_2$/NaCl]* compared with the uninhibited solution (ratio=0), as shown in Table 4.

Table 4 demonstrates that at a constant ratio of *[$NaNO_2$/NaCl]***,** the flow rate has no significant effect on the corrosion current density. This means that the reactions taking place in the passive region are not mass transfer dependent. The insignificant effect of flow on the corrosion current density leads to suggest that the passive film formation on the iron electrode is by an adsorption mechanism, which

is due to the nature of $NaNO_2$ especially if $NaCl$ is present. However, generally, it can be clearly noticed that the corrosion current density in inhibited solutions decreases with the increasing flow rate compared with the uninhibited solution (ratio=0). This can be attributed to the stability of the protective film formed on the metal surface. Therefore, the nitrite acts as an oxidizing agent and a stabilizer to the outer protective film.

Table 4. The corrosion current density×10^2, A/m^2.

rpm	[$NaNO_2$/NaCl]								
	0.0	0.3	0.4	0.5	0.6	0.7	0.8	0.9	1.0
0	96.257	7.326	2.941	1.978	4.064	3.850	7.487	1.737	2.500
200	160.43	10.695	4.598	3.208	3.208	2.139	4.278	2.540	2.406
350	229.95	1.657	6.400	3.743	0.428	5.348	4.813	0.484	0.802
500	262.03	5.722	4.064	3.743	5.561	2.460	3.850	3.797	3.00

In the anodic region, $NaNO_2$ behaves as an oxidizer. Therefore a stable passive film will be formed constituting Fe_3O_4 and γ-Fe_2O_3 on the outer side on the anodic sites blocking any further dissolution of iron [24]. The protective film comprises two layers, an inner Fe_3O_4 conductive film in direct contact with the metal, covered by an electrically insulating film of γ-Fe_2O_3. This is in agreement with the results obtained by Nagayama and Cohen [25], Bloom and Goldenberg [26], Kuroda *et al.* [27], Mayne and Pryor [28]. It is possibly formed through the adsorption of the nitrite ion followed by an oxidation step. The overall reaction is one or both of Eqs 1 and 2 [3, 15].

3.5 The Breakdown Point (D)

3.5.1 Breakdown Potential

The breakdown potential is important for the knowledge of the extent of the passivation. The passive state was terminated by a high polarization current indicating the onset of pitting corrosion. Usually, pitting at high polarization is associated with breakdown potential, Table 5.

Table 5. The breakdown potential of inhibited solution, V.

rpm	[$NaNO_2$/NaCl]							
	0.3	0.4	0.5	0.6	0.7	0.8	0.9	1.0
0	0.000	-0.020	0.000	0.060	0.240	0.120	1.000	0.280
200	0.060	0.000	0.120	0.200	0.660	0.160	0.320	0.260
350	0.080	0.000	0.000	0.040	0.360	0.140	0.240	0.060
500	0.020	0.060	0.180	0.160	0.400	0.140	0.200	0.300

After the film was broken, corrosion rate increased, assisting NO_2^- to be regenerated and reactivated, as shown in Eq 3. This caused the second passive film on the metal surface as shown by Eqs 1 and 2. However, this film has a less resistance compared with the complete passive region.

3.6 Inhibition Efficiency

The efficiency values were calculated by the following equation [29,30], Eq 4:

$$h\% = \frac{C.R._{(uninhibited)} - C.R._{(inhibited)}}{C.R._{(uninhibited)}} \times 100 \qquad 4$$

where i_{corr} for inhibited solution is taken as equal to the complete passive current density.

The results in Table 6 show that the protective films are too effective. Although, the best efficiencies were found at 0.9 for 0 rpm, 0.7 for 200, 500 rpm and 0.6 for 350 rpm, the other ratios are too high as well. Consequently, the best observation ratio must be found depending on the resistance of passive film layer which gives the best indication for the adequate used ratio.

Table 6. Inhibition efficiency (%).

rpm	[$NaNO_2$/NaCl]							
	0.3	0.4	0.5	0.6	0.7	0.8	0.9	1.0
0	92.389	96.945	97.945	95.778	96.000	92.222	98.195	97.403
200	93.334	97.134	98.000	98.000	98.667	97.333	98.417	98.500
350	99.279	97.217	98.372	99.814	97.674	97.907	99.789	99.651
500	97.816	98.449	98.572	97.878	99.061	98.531	98.551	98.855

3.7 The Resistance of Passive Film Layer

One of the main important factors in the protection of metals using inhibitors is the resistance of passive film layer. As mentioned before, the inhibition efficiency is too high due to the large difference between the current density before and after inhibition. Consequently, it is better to evaluate another trend to calculate and evaluate the best inhibition. Therefore, it was suggested a certain calculation for such purpose based on resistance of passive film layers. The resistance of passive film layer can be calculated as the ratio of the residual potential of passive film to the corrosion current; this is expressed in Eq 5:

$$R = \frac{E_b - E_{cp}}{i_{corr}} \qquad 5$$

where:

R : The resistance of passive film layer (Ω) (Hayyan equation).

$i_{corr.}$: Corrosion current density (A/m^2)

E_b : The breakdown potential (V).

E_{cp} : The complete passive potential (V).

Table 7 illustrates that the best resistance is at a molar ratio of 0.7 with 200 and 500 rpm. This is in agreement with previous studies [8, 9] which stated that the ratio of *$NaNO_2$/NaCl* must be about 0.7 in flow condition. However, at 350 rpm, although 0.7 is the widest range of potential for passive film layer but it can be observed that the best resistance ratio is 0.9. This is attributed to the wide range of passive film's potential in 0.9 in comparison to 0.6. In contrast, the inhibition efficiency shows 0.6 is best ratio because it has the lowest corrosion current density, Table 4. At static conditions the best protection ratio is 0.9 which can be attributed to the low concentration of *NaCl.* Hence, the ionization of the inhibitor may be lower than that at higher concentration; therefore, more inhibitor was needed to reach the best protection ratio.

Table 7. The resistance of passive film layer × 10^2 (per unit area m^2), Ω.

[$NaNO_2$/NaCl]	rpm			
	0	200	350	500
0.3	0.0273	0.0206	0.1689	0.0279
0.4	0.0680	0.0348	0.0125	0.0247
0.5	0.1112	0.0935	0.0374	0.0588
0.6	0.0443	0.0873	0.0935	0.0288
0.7	0.0571	0.2525	0.0860	0.2032
0.8	0.0401	0.0888	0.0582	0.0779
0.9	0.5181	0.1811	0.4545	0.0579
1.0	0.1440	0.1330	0.2494	0.0933

4. CONCLUSION

The effect of *$NaNO_2$* concentration on chloride ions in salt solution was investigated for the protection of carbon steel under controlled conditions of mass transfer using rotating cylinder electrode system. Potentiostatic polarization experiments were carried out at 313 K and rotational speeds of 0, 200, 350 and 500 rpm. For uninhibited and inhibited solutions, the concentration of chloride solution was 250 ppm *NaCl*. The experiments were conducted in the presence of *$NaNO_2$* with different concentrations depending on the *[$NaNO_2$/NaCl]* molar ratio, i.e. ratios of 0 to 1. A new calculation was suggested to obtain the best protection value depending on the resistance of passive film in the polarization curve. It was found that the best *[$NaNO_2$/NaCl]* protection molar ratio of carbon steel was 0.9 at 0 and 350 rpm whereas a value of 0.7 was achieved at 200 and 500 rpm. This reflected the nonlinear relationship between the rotor speed and the protection molar ratio. More investigation is

needed to explore other values of *NaCl* concentrations and develop a relationship for the effect of the operational conditions and salt concentration on the inhibition efficiency of $NaNO_2$.

ACKNOWLEDGMENTS
The authors thank the National Plan for Science, Technology, and Innovation at King Saud University for their financial assistance through project no. 10-ENV1010-02, University of Technology and University of Malaya for their support to this research.

References

1. P.R. Roberge, *Handbook of Corrosion Engineering*, McGraw-Hill, U.S.A. (2000).
2. A.W. Peabody, *Control of Pipeline Corrosion*, NACE International, U.S.A. (2001).
3. I. L. Rozenfeld, *Corrosion Inhibitors*, McGraw-Hill, New York (1981).
4. S.W. Dean, R. Derby and G.T. Bussche, *The Int. Corros. Forum*, 81 (1981) 253.
5. E.E. Stansbury and R.A. Buchanan, *Fundamentals of Electrochemical Corrosion*, ASM International (2000).
6. V.S. Sastri, *Corrosion Inhibitors, Principles and Application*, John Wiley (1998).
7. M. Marek, *Metals Handbook Corrosion*, Vol.13, 9th ed., ASM International (1987).
8. U.R. Evans, *The Corrosion and Oxidation of Metals*, Edward Arnold, London (1960).
9. P.K. Strivastavo, G.W. Kapse and A.K. Patwardhan, *Corrosion*, 37 (1981) 16.
10. J.J. Meyer, *Cracked Beam Testing*, American Engineering Testing, INC. (2003).
11. S. Matsuda, and H.H. Uhlig, *J. Electrochem. Soc.*, 111 (1964) 156.
12. A.D. Mercer, I.D.Jenkins and J.E.R. Brown, *Br. Corr. J.*, 3 (1968) 136.
13. J.F. Conoby and T.M. Swain, *Mat. Prot.*, 6 (1967) 55.
14. M. Cohen, *Corrosion*, 32 (1976) 46.
15. A. Marshall, *Corrosion Inhibitors for Use in Neutral Water System*, London, England, Oyez Scientific and services Ltd (1983).
16. C.P. Joseph, *Third Eur. Symp. Corr. Inhibitor*, University of Ferrara, P.791 (1971).
17. A.H. Rosemberge and J.M. Gaidis, *NACE*, 45 (1979).
18. C.P. Vazquez, Ph.D. Thesis, Univ. of Vigo (1999).
19. L.S. Van Delinder, *Corrosion Basics, An Introduction*, NACE (1984).
20. I. K. Salih, Ph.D. Thesis, U.O.T. (1993).
21. R.W. Lane, *Control of Scale and Corrosion in Building Water Systems*, McGraw-Hill, U.S.A. (1993).
22. A. AL-Borno, M. Islam and R. Haleem, *Corrosion*, 45 (1989) 990.
23. A.H. Ali, M.Sc. dissertation, U.O.T. (2002).
24. G. Hollander. and W.C. Ehrhard, *NACE*, (1982) 226.
25. M. Nagayama, and M. Cohen, *J. Electrochem. Soc.*, 109 (1962) 781.
26. M.C. Bloom and L. Goldenberg, *Corros. Sci.*, 5 (1965) 623.
27. K. Kuroda, B.D. Cahan, G. Nazri, E. Yeager and T.E. Mitchell, *J. Electrochem. Soc.*, 129 (1982) 2163.
28. J.E. Mayne and M.J. Pryor, *J. Chem. Soc.*, 7 (1949) 1831.
29. *Annual Book of ASTM Standards*, part 10, G31 (1980).
30. M.A. Pech-Canul and P. Bartolo-P`erez, *Surf. Coat. Technol.*, 184 (2004) 133.